InGaN RGB Light-Emitting Diodes With Monolithically Integrated Photodetectors for Stabilizing Color Chromaticity

Kwai Hei Li, *Member, IEEE,* Yuk Fai Cheung, Weijian Jin, Wai Yuen Fu, Albert Ting Leung Lee, *Member, IEEE,* Siew Chong Tan, *Senior Member, IEEE,* Shu Yuen Hui, *Fellow, IEEE,* and Hoi Wai Choi, *Senior Member, IEEE*

***Abstract*—In this paper, a solution toward realizing color chromaticity stabilized InGaN red, green, and blue (RGB) light-emitting diode (LED) is proposed and demonstrated. The InGaN/GaN multiple quantum wells (MQWs) play a key role in light emission from the LEDs and photodetection from the photodetectors (PDs). The spectral overlaps between the emission and absorption spectra are measured and the photocurrents of the PDs exhibit linear behavior with increasing LED driving currents. The solution involves the use of RGB chips with monolithically integrated PDs that detect the levels of light output from an individual chip in real time, whose photocurrent signals are fed to LED driver circuits that make use of the signal to provide a driving current that stabilizes the light output. Adoption of this feedback strategy results in CIE coordinates drifts of $\Delta(0.003, 0.005)$ over the 400 h duration of testing, proving to be an effective way of stabilizing color chromaticity from RGB LEDs.**

***Index Terms*—Color chromaticity, gallium nitride (GaN), light-emitting diode, monolithic integration, photodetector.**

I. Introduction

THE efficiencies and reliabilities of gallium nitride (GaN) light-emitting diode (LED)-based solid-state lighting are widely established. While LEDs have longer lifetimes than conventional lighting technologies [1]–[3], their performances degrade over time in the forms of reduction in luminous flux as well as shifts in chromaticity coordinates and color rendering index [4]–[6]. Even though all types of lamps experience color chromaticity shift to different extents, the long-term color stabilities (defined as the maintenance of spectral power distribution over time) of LEDs raise concerns owing to their significantly longer lifetimes [7], [8]. The effects of color shifts, which affect both the color appearance of the light source and the color of objects being illumination, depend on the application and the environment for which the light source is deployed. Generally, a high degree of color stability is required for high-end applications such as medical or museum lighting [9]–[11]. For applications involving large numbers of light sources, the lack of color stability will result in nonuniform color uniformities across the surfaces being illuminated.

There are two main types of LED-based white-light lighting in the market today. For general lighting applications, a color down-conversion material such as phosphor is coated onto a blue-light LED to produce a polychromatic spectrum [12]. For application requiring color tuning such as displays, a combination of red, green, and blue (RGB) LEDs is used. In either case, the color stabilities of LEDs depend on a variety of factors including driving current, ambient temperature, and heat-sinking [13], [14]. The emission spectrum of an LED comprising InGaN/GaN multiple quantum wells (MQWs) shifts with driving current due to the quantum confined Stark effect as well as carrier screening [15]. Heat accumulation at higher driving currents will also lead to bandgap shrinkage giving rise to spectral shifts, dependent on the ambient temperature and the heat-sinking capacity. This will be further affected by degradation of the phosphors in the color-converted emitters [16]. Given that color instabilities are inevitable and there is ample demand for high-quality color-stable lighting, solutions to counter color instabilities must be developed to improve the color characteristics of solid-state lighting in the long term.

Color control methods for RGB LED lighting system, considering the thermal characteristics of the devices, have previously been reported [17]–[19]. A direct optical approach to achieve color stability is to monitor the light output. In most cases, this involves stably mounting a photodetector (PD) or color sensor in front of the light source [20], [21], or through an optical beamsplitter, which might affect the compactness and robustness for which LED light sources are renown. With the collected readings, adjustments to the LED driving currents can be made to maintain preset color chromaticity. Color chromaticity shifts caused by phosphor degradation are tackled by the development of high stability phosphors and will not be dealt with in this paper. Instead, the focus will be on the maintenance of color chromaticity in RGB LEDs, which

Manuscript received February 11, 2019; revised May 8, 2019; accepted June 13, 2019. Date of publication July 9, 2019; date of current version February 10, 2020. This work was supported by the NFSC/RGC Joint Research Scheme sponsored in part by the Research Grants Council of Hong Kong and in part by the National Natural Science Foundation of China under Project N_HKU710/15. (Corresponding author: Hoi Wai Choi.)

The authors are with the Department of Electrical and Electronic Engineering, The University of Hong Kong, Hong Kong (e-mail: khli@eee.hku.hk; yfcheung@eee.hku.hk; weijianj@connect.hku.hk; wyfu@hku.hk; tlalee@eee.hku.hk; ronhui@eee.hku.hk; hwchoi@eee.hku.hk).

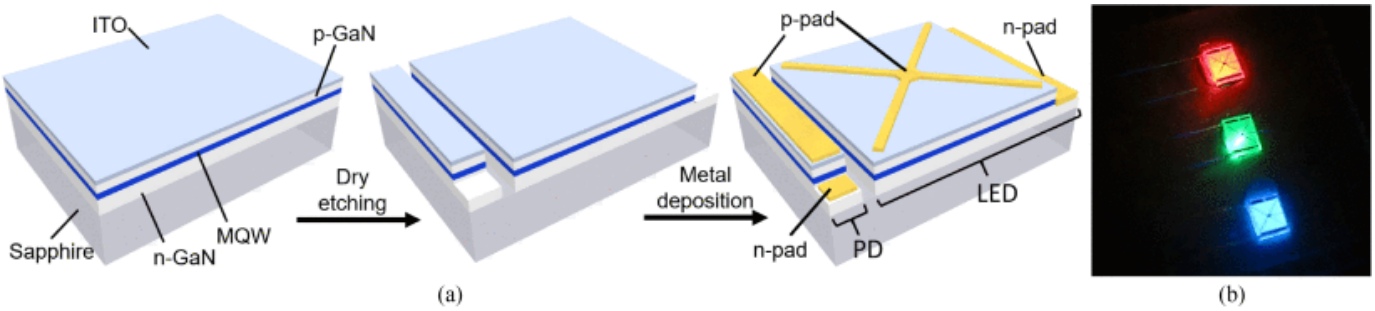

Fig. 1. (a) Schematic diagrams depicting the process flow of monolithically integrated PD-LED. (b) Microphotograph of RGB LEDs with monolithically integrated photodetectors.

involves maintenance of the color spectral distribution. The most direct way of doing so is the individual maintenance of luminous intensities from the RGB devices.

In this paper, we describe a method of monitoring the individual light output intensities of the LEDs in an InGaN RGB LED array using monolithically integrated PDs. The identical InGaN/GaN MQWs are not only responsible for light emission in the LED, but also used for photodetection in the PD. Being integrated on-chip without requiring addition regrowth, the PDs will sensitively detect light from the LED they are attached to on the same chip, while remaining insensitive to other LEDs or ambient lighting [22]. This detection scheme allows distinct monitoring of light from the individual RGB LEDs, while maintaining compactness and robustness of the lighting system. The detected photocurrents, representative of the light output intensities from the individual LEDs, are fed back to the LED driver which acts to stabilize the photocurrent, thus maintaining the light output. With stabilized light output across the RGB channels, the color chromaticity will also become stabilized.

II. Experimental Details

The LED wafers are grown by metal-organic chemical vapor deposition on 2-in patterned c-plane sapphire substrates, consisting of a 3 μm thick undoped GaN (u-GaN), 3 μm of Si-doped GaN (n-GaN), ten pairs of $In_xGa_{1-x}N$(5 nm)/GaN(12 nm) MQWs, capped with 200 nm of Mg-doped GaN (p-GaN). The blue, green, and red LED wafers correspond to $In_xGa_{1-x}N$ with x equal to 13%, 18%, and 26%, respectively. Processing of the wafers begin with the deposition of a 200 nm thick indium-tin-oxide current spreading layer over p-GaN as p-contact layer.

The LEDs and PDs are simultaneously fabricated on a single wafer using standard photolithography, dry etching, and contact-metallization techniques [22], as schematically shown in Fig. 1(a). A mesa of 1000×1000 μm^2, together with an adjacent mesa of 400×100 μm^2 with a separation of 100 μm, are photo-lithographically defined which function as LED and PD, respectively. The unmasked regions are etched down to expose the n-GaN surface by inductively coupled plasma (ICP) etching. The remaining GaN between the LED and PD is completely ICP-etched. Another photolithographic step is used to define the p-pad and n-pad regions and a bilayer of Ti/Au (40 nm/150 nm) is sequentially deposited by electron beam evaporation. The entire surface of the PD is metal-coated to minimize detection of ambient light. The chips are diced by laser micromachining and packaged on TO cans afterward to build an RGB LED, as shown in Fig. 1(b).

The electroluminescent (EL) spectra are obtained using an optical spectrometer comprising an Acton SP2500A 500 mm spectrograph and a Princeton Instrument PIXIS open-electrode CCD, while the spectral responsivities are measured with the same spectrometer by irradiating the devices with monochromatic light generated from a broadband light source dispersed through a monochromator.

III. Discussion

In these monolithically integrated LED-PD devices, the MQWs serve the dual functions of light emission in the LED and light detection in the PD. Fig. 2(a)–(c) show the electroluminescent spectra of the blue, green, and red LEDs operated at 5 mA, respectively, together with the normalized spectral responsivities of the on-chip PDs. The emission center wavelengths and spectral widths (FWHM), together with the spectral overlap between the emission and absorption spectra for the LEDs, are listed in Table I.

In all three devices, the on-chip PDs are capable of detecting light from their adjacent emitters with spectra overlap in the range of 34–36 nm. The photocurrents of the PDs increase monotonically with increasing driving currents to their corresponding on-chip LEDs as shown in Fig. 3, illustrating that the PDs can indeed be used to accurately monitor the light emission intensities of the corresponding on-chip LEDs. The plots in Fig. 2(a)–(c) also show that the extent of spectral overlap decreases from the blue to the red LED-PDs as the difference between emission and absorption referred to as the Stokes' shift enlarges with increasing indium incorporation in InGaN/GaN MQWs [23]. The red PD is thus capable of detecting light from the green and blue emitters, while the green PD can also detect emission from the blue LED, although each PD is supposed to only respond to light from its on-chip counterpart. This is circumvented by the deposition of a thick metal contact over the top surfaces of the PDs for light blocking, so that the majority of light detected by the PD is coupled from the on-chip LED through optical channeling in the transparent sapphire substrate and sidewall emission. The vertical sidewalls of the PDs are thus the only source of light leakage, although their surfaces areas are negligible. For

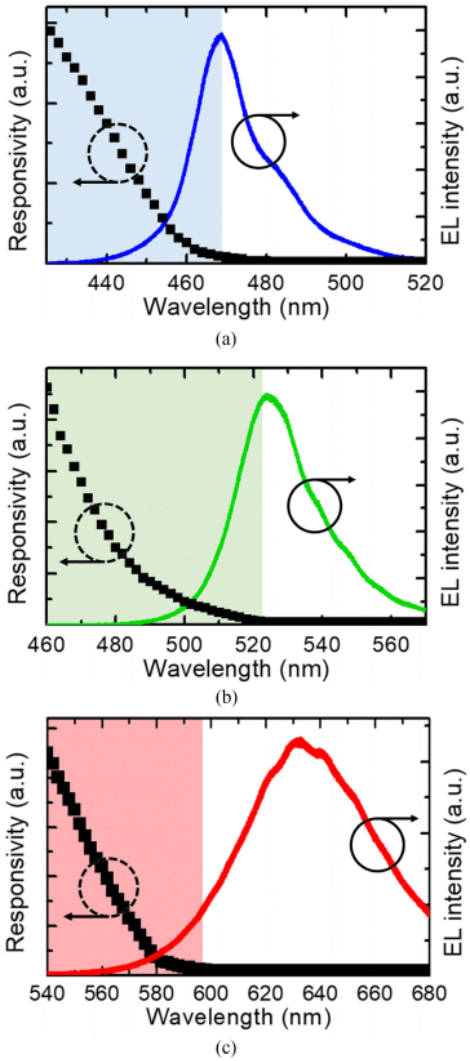

Fig. 2. Measured EL spectra of the (a) blue, (b) green, and (c) red LEDs operated at 5 mA and normalized spectral responsivities of the on-chip PDs.

TABLE I
EXPERIMENTAL RESULTS OF THE RBG LED-PD DEVICE

Device	Center wavelength (nm)	Spectral width (nm)	Spectral overlap (nm)
Blue LED/PD	470.2	18.7	36
Green LED/PD	526.5	24.3	35
Red LED/PD	636.2	50.6	35

the same reasons, the PDs have previously been found to be insensitive to ambient lighting [22], [24]. The photocurrents of the RGB PDs as functions of driving currents of the adjacent LEDs are also plotted in Fig. 3. It can be seen that while the blue and green PDs are insensitive to the light from the adjacent emitters, the red PD does generate a small photocurrent upon sensing blue and green light given its wider detection spectral range.

The schematic diagram (excluding the feedback circuits in grey bracket) in Fig. 4 shows the circuit setup for monitoring the light outputs of the RGB LEDs through their on-chip

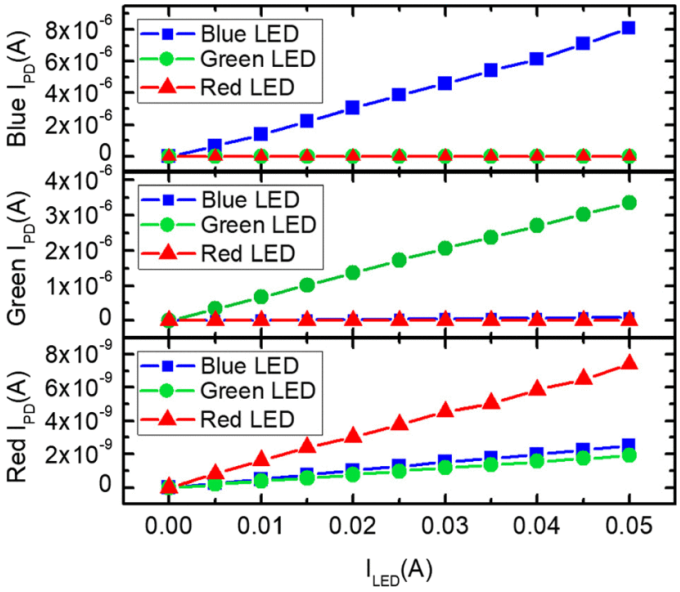

Fig. 3. Plot of photocurrent as a function of LED injection currents.

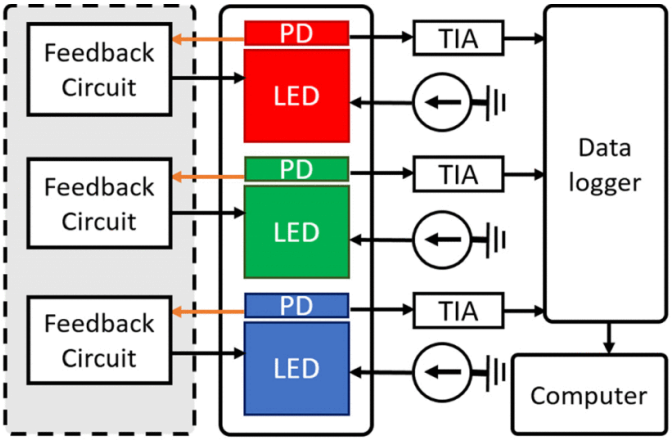

Fig. 4. Schematic diagram of experimental setup for regulating the light output from the RGB LEDs.

PDs. The LEDs, mounted within a dark enclosure to eliminate influences from the ambient, are driven with a benchtop power supply (Keithley 2230G-30-1). Since PDs generate currents, transimpedance amplifiers (TIAs) are used to amplify the small photocurrent signals into a much larger photovoltage signals. The voltage signals from on-chip PDs are collected by a data-logger (Picolog ADC-24).

The red, green, and blue LEDs are driven at 20, 1, and 0.8 mA, respectively, so that the nominal CIE coordinates of (0.21, 0.47) lie within the white region. Under normal laboratory conditions, the photovoltages of the red, green, and blue PDs over a period of 400 h at logging interval of 1 min are plotted in Fig. 5(a), together with the ambient temperature measured with a thermistor mounted within the dark enclosure, as well as the CIE coordinates measured by an externally calibrated colorimeter (Hopoocolor, OHSP-350C). It is found that the light outputs (photovoltages) of the red, green, and blue LEDs degrade by 0.4%, 17.4%, and 9.6% over the 400 h duration of logging while their signals fluctuate by

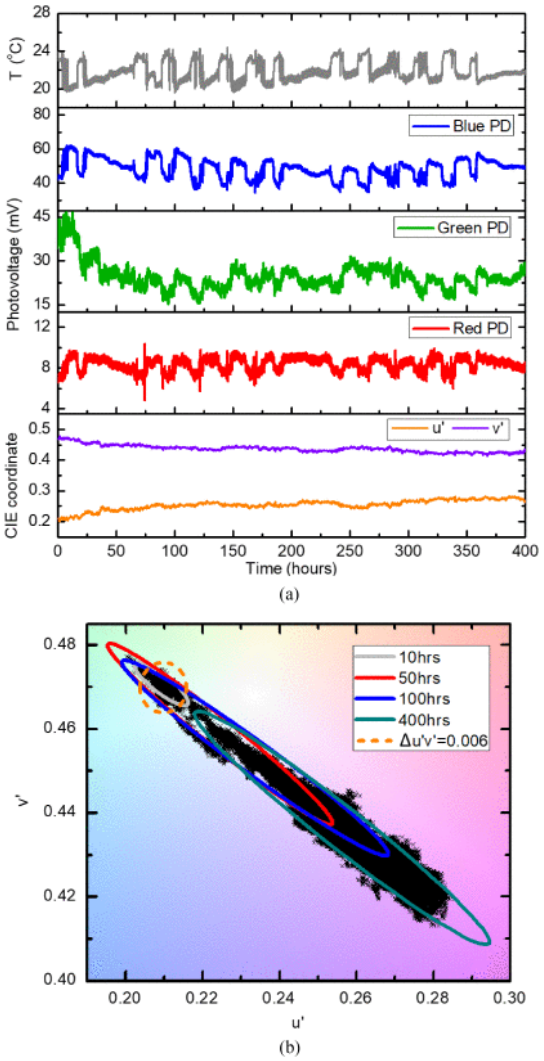

Fig. 5. (a) Plots of temperature, photovoltages of the on-chip RGB PDs, and CIE coordinates versus time. (b) CIE 1976 (u', v') chromaticity diagram showing the shift in color coordinates; ellipses show 95% confidence regions.

18.5%, 19.0%, and 18.7%, respectively, on average over 10 h periods, which causes a significant drift of CIE coordinates of $\Delta(0.014, 0.017)$ exceeding the tolerance of $\Delta u'v' = \pm 0.006$.

Although the variations in photovoltages track the variations in ambient temperatures closely, the color fluctuation is mainly due to different extents of intensity variations from individual RGB LEDs. As the on-chip PD is highly insensitive to temperature changes and provides a light-monitoring performance comparable to an external photosensor [22], the measured voltage signals can directly reflect the emitted light intensities of the LEDs. Moreover, initial rapid changes in light output intensities and color shifts followed by slow and more consistent changes are observed as the LEDs suffer certain degrees of burn-in effect during the initial operation period.

To further show the drifts of CIE coordinates over time, the ellipses covering approximately 95% of the scattered data points at different time periods are plotted in Fig. 5(b). The drifts of CIE coordinates widen over longer durations, as seen from the 95% confidence ellipse in Fig. 5(b). Additionally, the photovoltages of the red, green, and blue PDs fluctuate by 1.2%, 1.2%, and 0.4% over 1 h periods where temperature variations are mild; such fluctuations may be attributed to the statistical fluctuations in free charge carriers [25].

The ability to monitor the light output levels of individual LED devices of different emission wavelengths opens up the opportunity for color regulation. In order to demonstrate such capabilities, a peak current-mode controlled buck LED driver [26]–[28] is designed and implemented to regulate the flux intensities of these integrated LED-PD devices. By setting an external voltage reference, the flux will be well regulated at the desired level. A schematic diagram of the overall circuit is shown in Fig. 6(a).

This buck LED driver consists mainly of two parts, which are the power stage and the controller stage. For the power stage, a floating buck switching converter is applied. Unlike the classical buck converter with a high-side MOSFET, the floating buck switcher uses a low-side MOSFET (i.e., its source terminal is connected to ground). It can be driven directly by either a microcontroller or a simple low-side gate driver without additional bootstrap circuit. Thus, the implementation of the driving circuitry for this MOSFET can be much simplified. The LED portion of the integrated LED-PD device is the load end of the power stage. Since the topological states of the buck converter are already well discussed in the literature, they will not be repeated here. Current-mode control is used to regulate the LED current. By adjusting the ON-time duty ratio (D) of the main switch, which basically tracks with a fixed reference value of the luminous flux (V_{ref}), its average value can also be regulated, which is also the current that goes through the LED. As a result, the flux of the LED can be managed.

The PDs can be regarded as the beginning of the controller part of the circuit, which detects the flux of the LED to generate a sensed current. A TIA converts this sensed current to a proportional voltage level, which is more suitable and feasible to be measured and to control. In this way, the flux of the LED can be controlled indirectly by controlling the output of the TIA. This TIA signal is sent to the proportional-integral (PI) controller in the subsequent stage, together with a voltage reference level. The output of the PI controller will be compared with the sensed inductor current. Consequently, the comparator will generate a signal as the reset input of the set-reset (SR) latch. For this SR latch, its set input is connected to an external clock signal and its output is applied as the input of the driver for the MOSFET switch. When the clock signal is high, it will trigger the switch drive to turn ON the switch, so the inductor current will rise. Once the comparator gives a high level comparison result, which will trigger the reset function, the controller will turn OFF the MOSFET switch. When next rise level of the clock signal arrives, the switch will be turned ON again. Thus, the switching frequency of the buck converter will follow the frequency of the clock signal. Based on this logic, the turn-ON and turn-OFF period can be controlled, therefore, the average current passing through the LED and thus the flux intensity can be regulated.

In the hardware prototype, the PI controller is implemented by analog circuits, which include an OPA354 error amplifier,

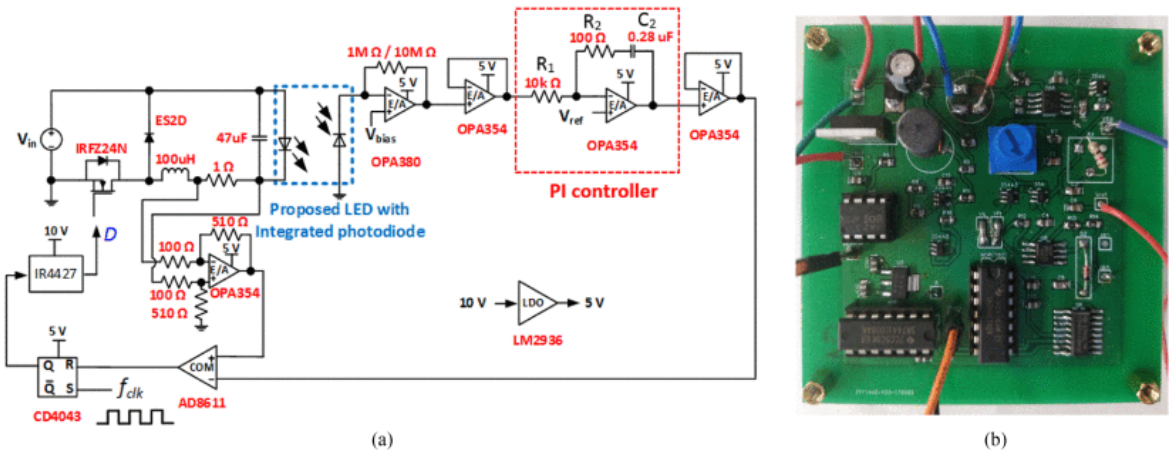

Fig. 6. (a) Circuit diagram and (b) photograph of feedback control circuit for regulating the output light intensity of an LED.

an integrator, and feedback resistors. In general, the transfer function of a PI controller is given by $G(s) = k_p + k_i/s = k_p + (k_p/T) \times (1/s)$, where k_p is the proportional gain, k_i is the integral gain, and T is the time constant. From simulation (using PSIM software), k_p is tuned to be 0.01 and the time constant T is approx. 28.5 µs, which is reasonably fast while producing stable response. Thus, the value of k_i can be determined to be around 250. In the analog-based PI controller, $k_p = R_2/R_1$ and $k_i = 1/(R_1C_2)$ [see Fig. 6(a)]. By choosing R_1 to be 10 kΩ, the values of R_2 and C_2 can be determined to be 100 Ω and 0.28 µF, respectively. Both the simulation and experimental results confirm that the PI controller can achieve precise current regulation of each RGB device based on the amplified photodiode current.

The significance of this peak current controlled buck LED driver is that when it is provided with a stable voltage reference, the driver will maintain the flux intensity at the desired level, avoiding influence by the ambience. For the RGB LED-PDs, each device has its own controller circuit according to its I–V characteristics so that the flux for each chip can be controlled independently. Even though the red PD may detect light from the adjacent blue and green LEDs, the emission from those LEDs have already been individually stabilized so that such photocurrents would be tiny and constant. The fluctuations of the photocurrent of the red PD would thus be primarily due to fluctuations in the light emission of the on-chip red LED. Although InGaN-based red LEDs are used in this paper, the same concept can be applied to AlGaInP-based red LEDs which are commonly found in commercial RGB LED packages. Like the InGaN/GaN MQWs, the AlGaInP/GaInP MQWs are also capable of both emitting and detecting light from the same chip, although the device fabrication process may differ slightly.

The plots of photovoltages from the RGB PDs in Fig. 7(a) clearly indicate stabilized light outputs from the RGB LEDs in spite of variations in ambient temperatures. Intensity variations over 10 h period reduce significantly to 0.26%, 0.10%, and 0.03%, respectively, resulting in highly stable CIE coordinates with drifts of less than $\Delta(0.001, 0.001)$. The drifts of measured CIE coordinates are within the maximum color tolerance

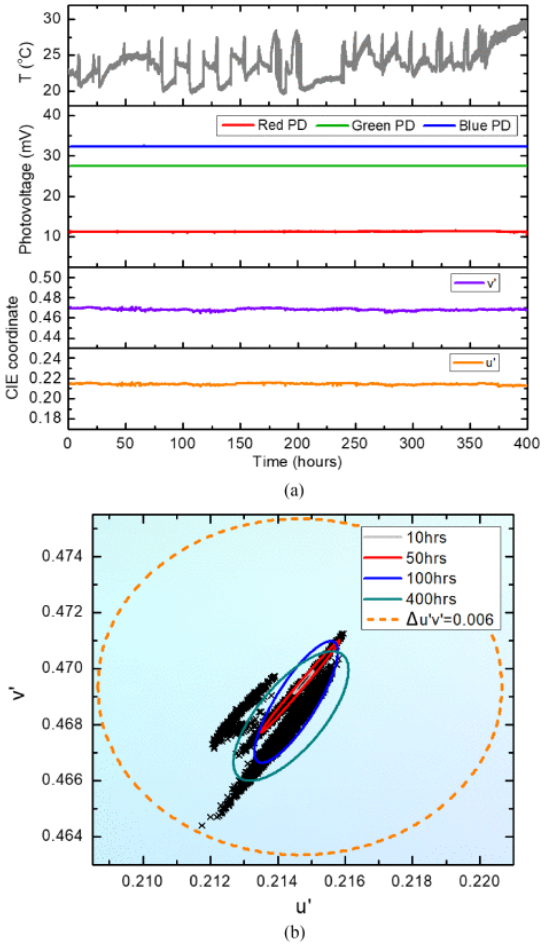

Fig. 7. (a) Plots of temperature, photovoltages of the on-chip RGB PDs, and CIE coordinates versus time with LEDs operated by feedback control circuits designed to regulate the light output. (b) CIE 1976 (u', v') chromaticity diagram; ellipses show 95% confidence regions.

of $\Delta u'v' = \pm 0.006$ according to ANSI Standard C78.377 [29] and only increases to $\Delta(0.003, 0.005)$ over 400 h period as seen from the ellipses in Fig. 7(b), verifying the feasibility of the proposed solution.

IV. Conclusion

In summary, a method of monitoring the individual light output intensities of the InGaN-based RGB LEDs using monolithically integrated PDs was demonstrated. The spectral overlaps between the emission and absorption spectra were measured and the PDs with identical MQWs were capable of sensitively detecting light from the LEDs. The detected photocurrents, representative of the light output intensities from the individual LEDs, were fed back to the LED drivers, which act to stabilize the photocurrent, thus maintaining the light output. With stabilized light outputs, intensity variations amongst RGB emitters over 10 h period significantly reduce from 18.5%, 19.0%, and 18.7% to 0.21%, 0.05%, and 0.59%, respectively, resulting in highly stable CIE coordinates with very small drifts of $\Delta(0.003, 0.005)$ over the 400 h duration of testing.

References

[1] M. H. Crawford, "Leds for solid-state lighting: performance challenges and recent advances," *IEEE Journal of Selected Topics in Quantum Electronics*, vol. 15, DOI 10.1109/JSTQE.2009.2013476, no. 4, pp. 1028–1040, 2009.

[2] E. F. Schubert and J. K. Kim, "Solid-state light sources getting smart," *Science*, vol. 308, DOI 10.1126/science.1108712, no. 5726, pp. 1274–1278, 2005.

[3] N. Narendran and Y. Gu, "Life of led-based white light sources," *Journal of Display Technology*, vol. 1, DOI 10.1109/JDT.2005.852515, no. 1, pp. 167–171, 2005.

[4] J. P. Freyssinier, M. R. Luo, N. Narendran, A. Bierman, and S. R. Pandharipande, "Mechanisms of color shift of high-power white-light led lamps," *Journal of Display Technology*, vol. 4, DOI 10.1109/JDT.2007.912361, no. 2, pp. 132–140, 2008.

[5] Y. Gu, N. Narendran, T. Dong, and H. Wu, "Spectral and luminous efficacy change of high-power leds under different dimming methods," *Proceedings of SPIE*, vol. 5530, DOI 10.1117/12.560318, pp. 129–137, 2004.

[6] C. K. Lee, Y. C. Cheng, and C. Y. Wu, "Investigation of lumen and color maintenance of high-power white light-emitting diodes," *IEEE Transactions on Device and Materials Reliability*, vol. 10, DOI 10.1109/TDMR.2009.2036754, no. 1, pp. 80–86, 2010.

[7] C. J. Humphreys, "Solid-state lighting," *MRS Bulletin*, vol. 33, DOI 10.1557/mrs2008.97, no. 4, pp. 459–470, 2008.

[8] J. Y. Tsao, M. H. Crawford, M. E. Coltrin, A. J. Fischer, D. D. Koleske, G. S. Subramania, G. T. Wang, J. J. Wierer, and R. F. Karlicek, "Toward Smart and Ultraefficient Solid-State Lighting," *Advanced Optical Materials*, vol. 2, DOI 10.1002/adom.201400119, no. 9, pp. 809–836, 2014.

[9] R. Y. Tsai, S. H. Chen, and C. H. Chen, "Colorimetric characterization of led lighting for museum applications," *Color Research & Application*, vol. 35, DOI 10.1002/col.20574, no. 4, pp. 271–278, 2010.

[10] A. M. Z. Slater, A. J. R. White, and P. R. Boyce, "The impact of spectral power distribution on the performance of tasks of medical importance," *Lighting Research & Technology*, vol. 41, DOI 10.1177/1477153508090569, no. 1, pp. 7–22, 2009.

[11] A. Cuttle, "A fresh approach to museum lighting," *Lighting Research & Technology*, vol. 39, DOI 10.1177/1477153507076157, no. 2, pp. 151–160, 2007.

[12] S. Nakamura and S. F. Chichibu, "Introduction to nitride semiconductor blue lasers and light emitting diodes," *Taylor & Francis*, 2000.

[13] K. A. F. Roelofs, H. P. Urbach, and K. A. M. de Groot, "Color point stability of white leds: temperature dependence," *Journal of Light & Visual Environment*, vol. 33, DOI 10.2150/jlve.33.122, no. 2, pp. 122–127, 2009.

[14] E. Carrasco and S. M. Sze, "Thermal effects on light-emitting diodes," *IEEE Transactions on Electron Devices*, vol. 15, DOI 10.1109/T-ED.1968.16569, no. 9, pp. 756–767, 1968.

[15] J. Piprek, "Efficiency droop in nitride-based light-emitting diodes," *Physica Status Solidi (A)*, vol. 207, DOI 10.1002/pssa.201026149, no. 10, pp. 2217–2225, 2010.

[16] Y. Narukawa, M. Ichikawa, D. Sano, T. Sakamoto, M. Sano, and T. Mukai, "Phosphor-conversion white light emitting diodes using ingan near-ultraviolet chip," *Japanese Journal of Applied Physics*, vol. 44, DOI 10.1143/JJAP.44.L1088, no. 21, pp. L1088–L1090, 2005.

[17] M. K. Kwon, S. H. Baek, J. Y. Kim, I. K. Park, and J. H. Kim, "Color stabilization of rgb light-emitting diodes by real-time monitoring of operating current and junction temperature," *Applied Physics Letters*, vol. 94, DOI 10.1063/1.3095595, no. 9, p. 091110, 2009.

[18] Y. Gu, N. Narendran, H. Wu, A. Freyssinier, and J. P. Freyssinier, "Spectral and luminous efficacy change of high-power leds under different dimming methods," *Proceedings of SPIE*, vol. 5530, DOI 10.1117/12.560318, pp. 129–137, 2004.

[19] D. A. Steigerwald, A. Bhat, D. Collins, R. Fletcher, M. Holcomb, M. Ludowise, P. Martin, and S. Rudaz, "Illumination with solid state lighting technology," *IEEE Journal of Selected Topics in Quantum Electronics*, vol. 8, DOI 10.1109/JSTQE.2002.1005894, no. 2, pp. 310–320, 2002.

[20] C. H. Lin and C. Y. Wu, "Digital color control for rgb led lighting using optical feedback," *IEEE Transactions on Industrial Electronics*, vol. 56, DOI 10.1109/TIE.2009.2012453, no. 3, pp. 737–745, 2009.

[21] K. T. Lam, K. H. Au, and K. W. Cheung, "Color control of rgb led lighting system using color sensors," *IEEE Transactions on Industrial Electronics*, vol. 60, DOI 10.1109/TIE.2012.2196896, no. 2, pp. 716–725, 2013.

[22] K. H. Li, W. Y. Fu, A. T. L. Lee, S. C. Tan, S. Y. Hui, and H. W. Choi, "Ingan light-emitting diodes with monolithically integrated photodetectors for real-time on-chip monitoring," *IEEE Photonics Journal*, vol. 9, DOI 10.1109/JPHOT.2017.2699222, no. 3, pp. 1–8, 2017.

[23] A. David, M. J. Grundmann, N. F. Gardner, J. Piprek, and S. Nakamura, "Carrier distribution in (0001) ingan/gan multiple quantum well light-emitting diodes," *Applied Physics Letters*, vol. 92, DOI 10.1063/1.2836813, no. 5, p. 053502, 2008.

[24] K. H. Li, W. Y. Fu, A. T. L. Lee, S. C. Tan, S. Y. Hui, and H. W. Choi, "Monolithically integrated ingan-based light-emitting diodes with photodetectors insensitive to ambient lighting," *Optics Letters*, vol. 42, DOI 10.1364/OL.42.004406, no. 21, pp. 4406–4409, 2017.

[25] A. Yariv and P. Yeh, "Photonics: Optical electronics in modern communications," *Oxford University Press*, 2006.

[26] S. C. Tan, Y. M. Lai, and C. K. Tse, "General design issues of led drivers for solid-state lighting," *IEEE Transactions on Industrial Electronics*, vol. 57, DOI 10.1109/TIE.2009.2028368, no. 5, pp. 1731–1739, 2010.

[27] S. C. Tan, Y. M. Lai, C. K. Tse, M. K. H. Cheung, and A. Ioinovici, "Adaptive dimming control of low-power led drivers based on the switching frequency modulation," *IEEE Transactions on Power Electronics*, vol. 24, DOI 10.1109/TPEL.2009.2022541, no. 9, pp. 2179–2189, 2009.

[28] S. Y. Hui, S. C. Tan, and H. H. C. Iu, "Led lamp circuit design with dimming capability," *IEEE Transactions on Power Electronics*, vol. 26, DOI 10.1109/TPEL.2010.2060375, no. 2, pp. 604–612, 2011.

[29] *ANSI C78.377-2017: Electric Lamps-Specifications for the Chromaticity of Solid-State Lighting Products*, American National Standards Institute Std., 2017.